DOI: 10.1002/ejic.200500883

A 3D Manganese Coordination Polymer $[Mn_3(IMDC)_2(H_2O)_4]$ Constructed from $[Mn_2(IMDC)_2(H_2O)_2]$ Layers and $[Mn(H_2O)_2]$ Pillars (IMDC = 4,5-imidazoledicarboxylate)

Man-Bo Zhang,[a] Yong-Mei Chen,[b] Shou-Tian Zheng,[a] and Guo-Yu Yang*[a]

Keywords: Carboxylate ligands / Coordination polymers / Hydrothermal synthesis / Manganese

A novel three-dimensional coordination polymer $[Mn_3(IMDC)_2(H_2O)_4]$ (**1**) (IMDC = 4,5-imidazoledicarboxylate), consisting of $[Mn_2(IMDC)_2(H_2O)_2]$ layers and $[Mn(H_2O)_2]$ pillars, was synthesized hydrothermally and characterized by IR spectroscopy, elemental analysis, TGA, and magnetic measurements. It is the first example of a 3D framework containing 4,5-imidazoledicarboxylate in the family of manganese complexes. Variable-temperature magnetic susceptibility measurements show a weak antiferromagnetic coupling interaction between the Mn^{II} ions of the dimeric units.

Introduction

Extended solids containing manganese and bridging ligands have been investigated widely in the past decades, mainly for use as molecule-based magnets in both fundamental and potential applications, especially those that exhibit spontaneous magnetization,[1,2] and in the synthesis of manganese metalloenzyme mimics in some biological redox-active systems,[3] as well as the intriguing varieties of architectures and topologies displayed by these compounds.[4,5] In the research area of metalloenzyme mimics, carboxylate-bridged systems are the focus of investigation. To date, many manganese complexes of carboxylic acids with six-membered heterocycles, such as 2,3-pyrazinedicarboxylic acid,[6] 2-pyrazinecarboxylic acid,[7] pyridine-2,6-dicarboxylic acid,[4,5] and pyridine-3,4-dicarboxylic acid[8] have been reported. However, the coordination chemistry of manganese and carboxylic acids with five-membered heterocycle is less developed. 4,5-Imidazoledicarboxylic acid (H_3IMDC) exhibits several interesting characteristics: a) it can be partially or completely deprotonated to generate H_2IMDC^-, $HIMDC^{2-}$, and $IMDC^{3-}$ by controlling the pH carefully, which allows 4,5-imidazoledicarboxylate anions to display various coordination modes;[9] b) the departure of carboxyl groups from the plane of the imidazole ring may allow 4,5-imidazoledicarboxylate to be used for the construction of helical structures; c) its six potential coordination donors allow the formation of interesting higher-dimensional structure. To the best of our knowledge, transition metal complexes of 4,5-imidazoledicarboxylate are usually either mononuclear,[10,11] dinuclear,[12] a 1D chain,[13,14] or a 2D layered network;[15] no 3D open framework is known. The typical coordination modes of 4,5-imidazoledicarboxylate anions are summarized in Scheme 1 (a–i). Herein, we report the synthesis, crystal structure, and magnetic properties of the first 3D coordination polymer of manganese with multidentate IMDC as ligand and linker, namely $[Mn_3(IMDC)_2(H_2O)_4]$ (**1**).

[a] State Key Laboratory of Structural Chemistry, Fujian Institute of Research on the Structure of Matter, Chinese Academy of Sciences,
Fuzhou, Fujian 350002, China
[b] Department of Applied Chemistry, Faculty of Science, Beijing University of Chemical Technology,
Beijing 100029, China
E-mail: ygy@fjirsm.ac.cn
Supporting information for this article is available on the WWW under http://www.eurjic.org or from the author.

Results and Discussion

Synthesis and Structure

As a few high dimensional coordination polymers of 4,5-imidazoledicarboxylic acid (H_3IMDC) have already been documented, we aimed to assemble the IMDC ligands and manganese ions into polymers with an open framework. In general, H_3IMDC is insoluble in water under neutral or acidic conditions at room temperature and is difficult to deprotonate under acidic conditions, which makes the construction of high-dimensional complexes difficult. In addition, although the sodium salt of 4,5-imidazoledicarboxylate is soluble in water, it easily forms precipitates, rather than crystals, in the presence of manganese ions. Taking into account the above two aspects, we chose the insoluble manganese salt $MnCO_3$ as starting material, with an $H_3IMDC/MnCO_3$ molar ratio of 2:1, and heated the mixture hydrothermally at 175 °C for 15 days, expecting that the insoluble $MnCO_3$ should slow the reaction down and allow the H_3IMDC time to deprotonate. We also carried

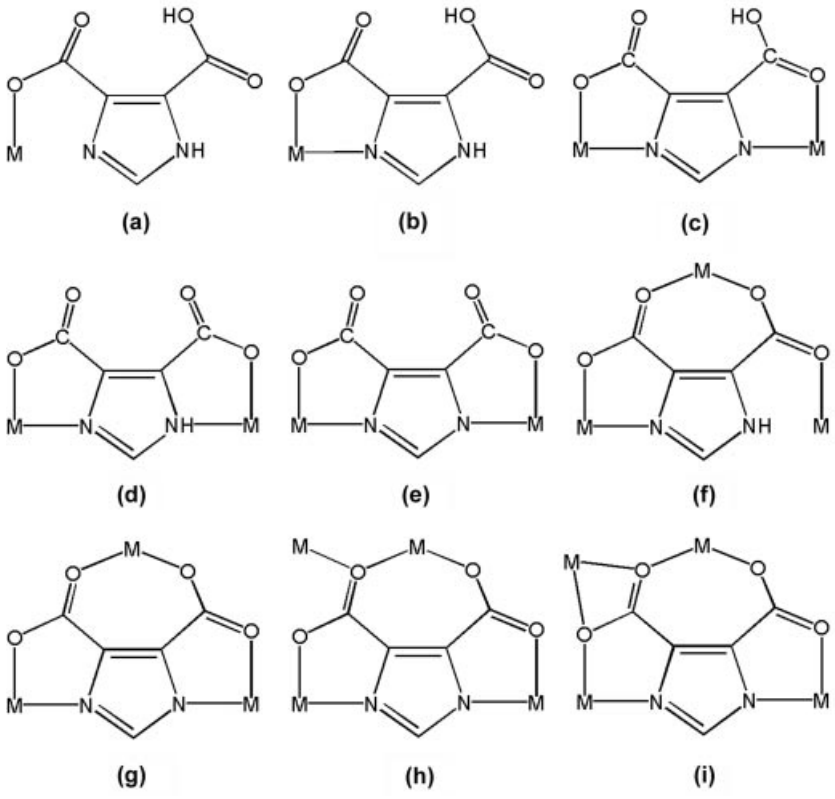

Scheme 1. Typical coordination modes of the IMDC ligand.

out the same reaction in a period shorter than 10 days, but no crystals were obtained. Thus, the slower rate and longer time may be crucial factors for the crystallization of **1**.

X-ray analysis revealed that the asymmetric unit consists of two crystallographically independent Mn^{2+} centers, one IMDC ligand, and two coordinated water molecules (Figure S1, see Supporting Information). The coordination mode of the IMDC in **1** is illustrated in Scheme 1 (h) and Figure S2 in the Supporting Information. The coordination environments of the Mn(1) and Mn(2) atoms and the IMDC ligand in the symmetric unit are presented in Figure 1. Both Mn(1) and Mn(2) are six coordinated to form two octahedra, $Mn(1)NO_4(H_2O)$ and $Mn(2)N_2O_2(H_2O)_2$. In the $Mn(1)NO_4(H_2O)$ moiety the six donors are one N atom of an imidazole ring, one water molecule, and four O atoms of four carboxylate groups, with one in mode A, two in mode B, and one in mode C (Scheme 1), while in $Mn(2)N_2O_2(H_2O)_2$ the donors are two N atoms from two IMDC ligands, two water molecules, and two O atoms of two carboxylate groups (mode A). As for the IMDC ligand, the carboxyl groups bonds to four Mn atoms in four different coordination modes:[16] a μ_2-carboxylato-*syn-anti* mode for Mn(1)–O(1)–C(1)–O(2)–Mn(1d), a μ_2-carboxylato-*anti-anti* mode for Mn(1)–O(1)–C(1)–O(2)–Mn(1e), a μ_2-carboxylato-*anti-anti* mode for Mn(2)–O(4)–C(4)–O(3)–Mn(1e), and a bis(μ_2,η^1-carboxylato) mode for Mn(1d)–O(2)–Mn(1e) (see Figure S2).

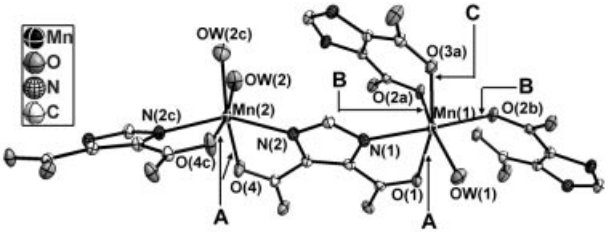

Figure 1. ORTEP drawing (ellipsoids at 50% probability) with the atom-labeling scheme for the symmetric unit of complex **1**. The labels "a" or "b" refer to symmetry-generated atoms and the labels "A", "B", and "C" refer to the different binding modes of the carboxylate groups of then IMDC ligand.

Although both Mn(1) and Mn(2) are six-coordinate, the different coordination environments around them result in an Mn(1) dimer and Mn(2) monomer (Figure S3). In the dimer, the O(2) atom from a mode-B carboxylate group bonds two Mn(1) centers to form the dimeric unit $Mn_2(IMDC)_2(H_2O)_2$ [Mn(1)–O(2) = 2.169 Å] whose Mn···Mn distance is 3.477 Å; the O–Mn–O angle in the Mn_2O_2 ring is 75.46°, while the Mn–O–Mn angle is 104.54°. These values fall in the range of similar dinuclear manganese complexes.[17–19] In the structure, each $Mn_2(IMDC)_2(H_2O)_2$ dimer further connects to adjacent dimeric units through O(1) from a mode-A carboxylate group and N(1) atoms to form a 2D layer in the *ab* plane (Figures 2 and 3).

It is worth noting the presence of left- and right-handed helical chains consisting of repeating –Mn(1)–O(2)–C(1)–O(1)– linkages in the layer along the [100] direction (Figures 3 and S4). O(4) from a mode-A carboxylate group and the N(2) atoms coordinate to the Mn(2) center to give rise to the 3D open framework (Figures 4 and S5). In other words, the Mn(1) centers mainly contribute to constructing the layers together with IMDC ligand, while the Mn(2) centers act as pillars between the layers.

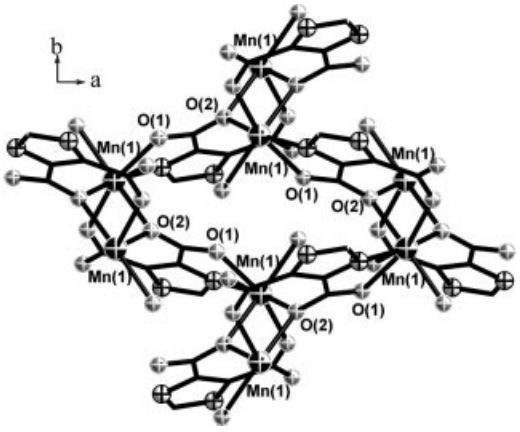

Figure 2. Layer containing $Mn_2(IMDC)_2(H_2O)_2$ dimers.

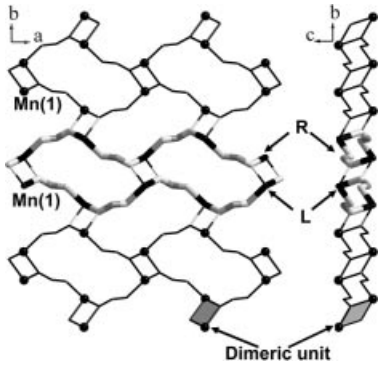

Figure 3. View of the layer constructed by $Mn_2(IMDC)_2(H_2O)_2$ dimers along the *c* and *a* axis; the imidazole rings of IMDC ligands have been omitted for clarity; L and R indicate the left- and right-handed helical chains. The thick, two-colored line represents the helical chains in the *ab* plane.

The H_3IMDC is completely deprotonated in compound **1**, and all six potential donor atoms coordinate to four Mn centers through coordination mode h of Scheme 1, which plays a key role in constructing the 3D framework of **1** (Figure S1). The previously reported coordination modes of the IMDC ligand, i.e. modes a and b of Scheme 1, can only coordinate to one metal center, thus monomers are the favorable entity to accommodate them.[10,11] As for coordination modes c, d, and e, they can link two metal centers through two chelating five-membered rings on the opposite side of the imidazole group to form a linear bridge. For example, if the IMDC ligands connect the metal centers along one direction, chain-like structures are formed as in [Mn(phen)(HIMDC)][13] and $[Cd(HIMDC)(H_2O)_2]$[14] (Figure S6a), whereas if the ligands connect the metal

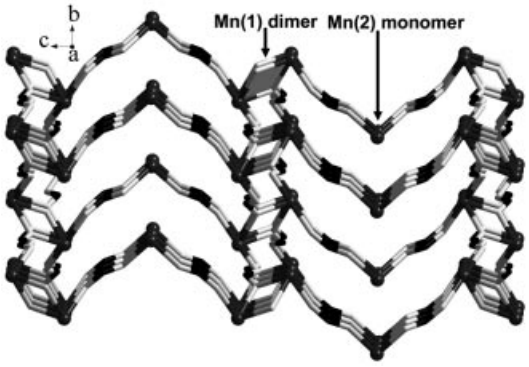

Figure 4. View of the 3D framework constructed by 2D layers containing Mn(1) atoms and pillars consisting of Mn(2) atoms.

centers perpendicularly, a square tetramer, as in $[Na_2\{Co^{II}_2Co^{III}_2(IMDC)_4(bipy)_4\}]\cdot 12H_2O$[20] (Figure S6b) or a cubane-like $[Ni_8(HIMDC)_{12}]^{8-}$ cluster unit, as in $[Ni_8(HIMDC)_{12}(H_2TMDP)_4(DMF)_4(EtOH)_4(H_2O)_6]$[21] (Figure S6c) are formed. Mode f in Scheme 1 tends to yield a 2D layered network.[15] In the structures of a series of lanthanide complexes $[Ln_2(IMDC)_2(H_2O)_3]\cdot nH_2O$,[9] the IMDC ligands displays modes g and i: in the g mode they connect three lanthanide atoms to form a 1D helical channel, while in the i mode they contribute to connecting the helical channels to form a 3D framework. From the above discussion, we can conclude that multidentate modes of the IMDC ligand, such as g, h, and i, benefit the formation of higher-dimensional frameworks.

IR Spectrum and Thermal Stability Analysis

The absence of any strong bands around 1700 cm^{-1} in the IR spectrum of **1** indicates that 4,5-imidazoledicarboxylic acid has been completely deprotonated to generate $IMDC^{3-}$ anions. The sharp bands in the region 1581–1541 cm^{-1} may be attributed to the COO^- asymmetric stretching modes, and the bands at 1384 cm^{-1} are characteristic of the symmetric stretching modes of COO^- (Figure S7). The value of the difference $\Delta(\nu_{as} - \nu_s)$ between the two stretching modes is about 197 cm^{-1}, which indicates strong coordination of the carboxylate oxygen to the manganese center. In contrast to **1**, the presence of a medium intensity band in the region 1730–1710 cm^{-1} in the IR spectrum of *cis*-$[Ru(PPh_3)_2(L^3H_2)_2]$ ($L^3H_2 = H_2IMDC$) suggests that the 4,5-imidazoledicarboxylic acid is only partially deprotonated.[22]

The TG curve shows that the structure is stable up to 210 °C, and the weight loss of complex **1** can be divided into three steps in the range 210–1000 °C (Figure S8). The weight loss of 13.5 % during the first step from 210 to 350 °C corresponds to the loss of four coordinated water molecules (calcd. 13.3 %). On further heating, the material loses weight continuously during the second and the third steps, with the combined weight loss of 47.3% (calcd. 47.5%) corresponding to decomposition of the IMDC ligand. Assuming the residue is MnO, the observed weight

(38.8%) is in good agreement with the calculated value (39.2%).

Magnetic Properties

Temperature-dependent magnetic susceptibility measurements for complex **1** were performed over a temperature range from 5 to 300 K at 5 kOe. The magnetic susceptibility above 6 K obeys the Curie–Weiss law and gives a Curie constant, C, of 13.6 $cm^3 K mol^{-1}$ and a Weiss constant, θ, of –14.1 K. The value of C is in agreement with that expected for three magnetically isolated Mn^{2+} ions with $S = 5/2$ (13.1 $cm^3 K mol^{-1}$; $g = 2$). Upon cooling, the value of $\chi_M T$ decreases monotonically, attaining a value of 3.0 $cm^3 K mol^{-1}$ at 5 K. Such behavior is characteristic of the presence of weak antiferromagnetic interactions between the neighboring Mn^{2+} ions (Figure 5).

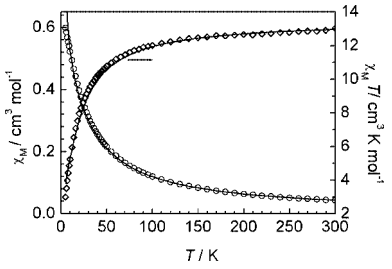

Figure 5. Plot of the $\chi_M T$ product and χ_M versus T for complex **1**. The solid lines represent the best fit to the model with inclusion of the ZFS term.

From the known structural data, there are four types of Mn···Mn exchange pathways via the carboxylate groups in the structure (Figure S2). As the Mn···Mn distance of 3.477 Å within the bis(μ_2,η^1-carboxylato)-bridged bimetallic Mn_2O_2 core is much shorter than the Mn···Mn separations of 5.60–6.52 Å through μ_2-1,3-carboxylato modes (in *anti-anti*/*syn-anti*) or an IMDC bridge, and the latter is generally less capable of transmitting magnetic interactions,[13,23–26] we can simplify the coupling interaction system as a doubly μ_2,η^1-carboxylato-bridged dimeric manganese combining an isolated $Mn(2)^{2+}$ ion. The magnetic behavior of the compound is therefore approximated by the sum of the contributions of one Mn^{2+} dimer (Bleaney–Bowers-like equation based on the isotropic Heisenberg model $H = -2JS_1 \cdot S_2$)[27] and one isolated Mn^{2+} ion, in which a Weiss constant, θ', is included to describe the interdimer interactions and the exchange coupling between Mn1 and Mn2 is neglected. The corresponding analytical expression for the $\chi_M T$ product is given as follows [Equations (1), (2), and (3)].

$$\chi_M T = \chi_{dimer} T + \chi_{mono} T \quad (1)$$

where

$$\chi_{dimer} = \frac{2Ng^2\beta^2}{k(T-\theta)} \times \left[\frac{e^x + 5e^{3x} + 14e^{6x} + 30e^{10x} + 55e^{15x}}{1 + 3e^x + 5e^{3x} + 7e^{6x} + 9e^{10x} + 11e^{15x}} \right]$$

$$x = 2J/kT \quad (2)$$

and

$$\chi_{mono} = \frac{Ng^2\beta^2 S(S+1)}{3kT} \quad (3)$$

in which N, g, k, and β have their usual meanings, and J is the exchange coupling constant between the doubly μ_2,η^1-carboxylato-bridged manganese ions. The fitting using Equation (1) gave a satisfactory result above 10 K with the superexchange parameters $J = -1.34\ cm^{-1}$, $\theta' = -7.40$ K, and $g = 2.03$. The agreement factor R, defined as $\Sigma[(\chi_M T)_{obs} - (\chi_M T)_{calc}]^2/\Sigma(\chi_M T^2_{obs})$ is equal to 1.85×10^{-3}. These values confirm the antiferromagnetic character of the magnetic interaction between the Mn^{2+} ions via double μ_2,η^1-carboxylato bridges. The deviation below 10 K may arise from the neglect of the coupling interactions involving the Mn(2) ion or its zero-field splitting (ZFS).

When the zero-field splitting (D) of the Mn(2) ions is considered by using the theoretical expression[28] for an $S = 5/2$ spin instead of Equation (3), a better agreement between the observed and calculated $\chi_M T$ value at low temperature is found with the four-parameter fits than with the three-parameter fit. However, the parameters D and θ' are strongly dependent on each other, therefore it is difficult to calculate these values with reasonable accuracy. If the values of J, g, and θ' are constrained to the value obtained by the simplified expression based on Equations (2) and (3), the best fitting based on the model with inclusion of ZFS term yields $D = 7.89\ cm^{-1}$ with $R = 5.4 \times 10^{-4}$. The D value is obviously larger than those observed in similar systems,[29,30] suggesting that there are still some disparities between the present magnetic model and the actual magnetic interaction system. The small J value ($-1.34\ cm^{-1}$) indicates weak antiferromagnetic coupling in the dimeric units of complex **1**, which is comparable to the values found in the doubly μ_2,η^1-carboxylato-bridged manganese complexes (-0.631 to $-0.942\ cm^{-1}$).[19,25] Due to a shorter Mn···Mn distance (3.477 Å), the J value of **1** is slightly larger than those of the above mentioned manganese complexes (3.67–3.73 Å).

Conclusion

In summary, we have synthesized a novel 3D Mn-IMDC coordination polymer under hydrothermal conditions. The structure is constructed from $[Mn(H_2O)_2]$ pillars and $[Mn_2(IMDC)_2(H_2O)_2]$ layers containing left- and right-handed helical chains. The 4,5-imidazoledicarboxylic acids are completely deprotonated and adopt coordination mode h of Scheme 1. Compared with the coordination modes shown in this scheme, mode h allows the 4,5-imidazoledicarboxylate ligand to form a high dimensional framework. The TG curve shows **1** is very stable below 210 °C and the magnetic measurement of **1** indicates the presence of weak antiferromagnetic exchange interactions.

Experimental Section

General Remarks: 4,5-Imidazoledicarboxylic acid (H_3IMDC) and $MnCO_3$ were purchased from commercial sources and used as received. Elemental analysis (C,H,N) was carried out with a Vario EL III elemental analyzer. IR spectra (400–4000 cm^{-1}) were recorded from KBr pellets on an ABB Bomem IR MB102 series spectrophotometer. The thermogravimetric analysis was performed with a Mettler Toledo TGA/SDTA 851e analyzer in N_2 with a heating rate of 10 °C min^{-1} from 30 to 1000 °C. The variable-temperature magnetic susceptibility measurement of a crystalline sample was performed in a field of 5 kOe with a Quantum Design MPMS-7 magnetometer; the susceptibility of the sample holder and diamagnetic contribution were subtracted from the raw data for the complexes.

Synthesis and Initial Characterization: A mixture of H_3IMDC (0.2341 g, 1.5 mmol), $MnCO_3$ (0.0862 g, 0.75 mmol), and H_2O (5 mL; $MnCO_3/H_3IMDC/H_2O$ molar ratio of 1:2:370) was stirred under ambient conditions. The resulting mixture with a pH of 4 was sealed in a 25-mL Teflon-lined steel autoclave and heated at 175 °C for 15 d under autogenous pressure. After cooling to room temperature, the colorless prismatic crystals of **1** were filtered off, washed with distilled water, and dried at ambient temperature (39 mg, yield 28.7% based on $MnCO_3$). $C_{10}H_{10}Mn_3N_4O_{12}$ (543.04): calcd. C 22.12, H 1.86, N 10.33; found C 22.20, H 2.01, N 10.35. IR (KBr pellet): $\tilde{\nu}$ = 3542 (s) cm^{-1}, 3280 (s), 1662 (m), 1581 (s), 1515 (vs), 1409 (vs), 1384 (vs), 1276 (m), 1241 (s), 1107 (m), 1099 (m), 803 (m), 671 (m).

X-ray Crystallographic Study: A crystal of dimensions $0.35 \times 0.18 \times 0.15$ mm^3 was used for data collection on a Siemens Smart CCD diffractometer with graphite-monochromated Mo-K_α radiation (λ = 0.71073 Å). Of the 8895 reflections ($2\theta_{max}$ = 50.04°), 1422 were independent (R_{int} = 0.0199) and 1396 reflections with $I > 2\sigma(I)$. The structure of **1** was solved by direct methods and all calculations were performe with the SHELXL program and refined by full-matrix, least-squares minimizations of $(F_o - F_c)^2$ with anisotropic thermal parameters for all non-hydrogen atoms. The position of the hydrogen atoms were found in the difference Fourier maps and refined isotropically. The last successful full-matrix least-squares refinement with anisotropic thermal parameters for all non-hydrogen atoms converged to R_1 = 0.0226, wR_2 = 0.0640. Experimental details for X-ray data collection of **1** are presented in Table 1, while selected bond lengths and angles are listed in Table 2.

Table 1. Crystal data and structure refinement for complex **1**.

Empirical formula	$C_{10}H_{10}Mn_3N_4O_{12}$
Formula weight	543.04
Crystal system	orthorhombic
Space group	*Pbcn*
a [Å]	9.386
b [Å]	7.351
c [Å]	23.3442(17)
V [Å^3]	1610.78(12)
Z	4
μ(Mo-K_α) [mm^{-1}]	2.396
T [K]	293(2)
ρ_{calc} [g cm^{-3}]	2.239
λ [Å]	0.71073
F(000)	1076
θ range for data collection	1.74–25.02°
Reflections collected/unique	8895/1422 [*R*(int) = 0.0199]
Goodness-of-fit on F^2	1.016
Final *R* indices [$I > 2\sigma(I)$]	$R1$ = 0.0226[a] $wR2$ = 0.0640[b]
R indices (all data)	$R1$ = 0.0252, $wR2$ = 0.0922
Largest diff. peak and hole [e Å^{-3}]	0.369 and –0.332

[a] $R1 = \Sigma(||F_o| - |F_c||)/\Sigma|F_o|$. [b] $wR2 = \{\Sigma[w(F_o^2 - F_c^2)^2]/\Sigma[w(F_o^2)^2]\}^{1/2}$, where $w = 1/[\sigma^2(F_o)^2 + (0.0506P)^2 + 5.0080P]$ where $P = (F_o^2 + 2F_c^2)/3$.

Table 2. Selected bond lengths [Å] and angles [°] for complex **1**.[a]

Mn(1)–O(3A)	2.126(2)	Mn(2)–N(2C)	2.181(2)
Mn(1)–O(2B)	2.169(2)	Mn(2)–N(2)	2.181(2)
Mn(1)–OW1	2.180(2)	Mn(2)–OW(2C)	2.215(3)
Mn(1)–O(1)	2.205(2)	Mn(2)–OW(2)	2.215(3)
Mn(1)–N(1)	2.213(2)	Mn(2)–O(4)	2.241(2)
Mn(1)–O(2A)	2.228(2)	Mn(2)–O(4C)	2.241(2)
O(3A)–Mn(1)–O(2B)	90.3(1)	O(1)–Mn(1)–O(2A)	85.8(1)
O(3A)–Mn(1)–OW(1)	107.8(1)	N(1)–Mn(1)–O(2A)	93.7(1)
O(2B)–Mn(1)–OW(1)	92.7(1)	N(2C)–Mn(2)–N(2)	150.6(1)
O(3A)–Mn(1)–O(1)	163.6(1)	N(2)–Mn(2)–OW(2C)	102.7(1)
O(2B)–Mn(1)–O(1)	98.7(1)	OW(2C)–Mn(2)–OW(2)	85.1(2)
OW(1)–Mn(1)–O(1)	85.6(1)	N(2C)–Mn(2)–O(4)	88.8(1)
O(3A)–Mn(1)–N(1)	93.3(1)	N(2)–Mn(2)–O(4)	73.7(1)
O(2B)–Mn(1)–N(1)	168.2(1)	OW(2C)–Mn(2)–O(4)	168.0(1)
OW(1)–Mn(1)–N(1)	96.9(1)	OW(2)–Mn(2)–O(4)	84.2(1)
O(1)–Mn(1)–N(1)	75.3(1)	N(2C)–Mn(2)–O(4C)	73.7(1)
O(3A)–Mn(1)–O(2A)	83.2(1)	N(2)–Mn(2)–O(4C)	88.9(1)
O(2B)–Mn(1)–O(2A)	75.5(1)	N(2)–Mn(2)–OW(2)	98.8(1)
OW(1)–Mn(1)–O(2A)	164.2(1)	O(4)–Mn(2)–O(4C)	107.0(1)

[a] Symmetry transformations used to generate equivalent atoms: A: $-x - 3/2$, $y - 1/2$, z; B: $x + 1/2$, $-y + 1/2$, $-z + 1$; C: $-x - 2$, y, $-z + 1/2$.

CCDC-258312 contains the supplementary crystallographic data for this paper. These data can be obtained free of charge from The Cambridge Crystallographic Data Centre via www.ccdc.cam.ac.uk/data_request/cif.

Supporting Information (see footnote on the first page of this article): Eight additional figures including the IR spectrum and TG curve are available.

Acknowledgments

This work was supported by the National Natural Science Foundation of China (grant nos. 20271050 and 20473093), the Talents Program of the Chinese Academy of Sciences, and the Natural Science Foundation of Fujian Province (grant nos. E0510030 and E0210029).

[1] S. Wang, G. Yang, D. Liao, L. Li, *Inorg. Chem.* **2004**, *43*, 852–854.
[2] H.-J. Chen, Z.-W. Mao, S. Gao, X.-M. Chen, *Chem. Commun.* **2001**, 2320–2321.
[3] G. C. Dismukes, *Chem. Rev.* **1996**, *96*, 2909–2926.
[4] B. Zhao, P. Cheng, Y. Dai, C. Cheng, D. Liao, S. Yan, Z. Jiang, G. Wang, *Angew. Chem. Int. Ed.* **2003**, *42*, 934–936.
[5] B. Zhao, P. Cheng, X. Chen, C. Cheng, W. Shi, D. Liao, S. Yan, Z. Jiang, *J. Am. Chem. Soc.* **2004**, *126*, 3012–3013.
[6] J.-Z. Zou, Z. Xu, W. Chen, K.-M. Lo, X.-Z. You, *Polyhedron* **1999**, *18*, 1507–1512.
[7] J. Limburg, G. W. Brudvig, R. H. Crabtree, *J. Am. Chem. Soc.* **1997**, *119*, 2761–2762.
[8] W. Chen, Q. Yue, C. Chen, H. M. Yuan, W. Xu, J. S. Chen, S. N. Wang, *Dalton Trans.* **2003**, 28–30.
[9] Y.-Q. Sun, J. Zhang, Y.-M. Chen, G.-Y. Yang, *Angew. Chem. Int. Ed.* **2005**, *44*, 5814–5817.
[10] C. Ma, F. Chen, C. Chen, Q. Liu, *Acta Crystallogr., Sect. C* **2003**, *59*, m516–m518.

[11] Y. L. Wang, R. Cao, W. H. Bi, *Acta Crystallogr., Sect. C* **2004**, *60*, m609–m611.
[12] M. T. Caudle, J. W. Kampf, M. L. Kirk, P. G. Rasmussen, V. L. Pecoraro, *J. Am. Chem. Soc.* **1997**, *119*, 9297–9298.
[13] X. Zhang, D. Huang, F. Chen, C. Chen, Q. Liu, *Inorg. Chem. Commun.* **2004**, *7*, 662–665.
[14] Y.-Q. Sun, J. Zhang, G.-Y. Yang, *Acta Crystallogr., Sect. C* **2004**, *60*, m590–m591.
[15] S. Gao, L. Huo, H. Zhao, J. Liu, *Acta Crystallogr., Sect. E* **2005**, *61*, m155–m157.
[16] R. L. Rardin, W. B. Tolman, S. J. Lippard, *New J. Chem.* **1991**, *15*, 417–430.
[17] C. Policar, S. Durot, F. Lambert, M. Cesario, F. Ramiandrasoa, I. Morgenstern-Badarau, *Eur. J. Inorg. Chem.* **2001**, *40*, 1807–1818.
[18] C. Ma, C. Chen, Q. Liu, D. Liao, L. Li, *Eur. J. Inorg. Chem.* **2003**, *42*, 1227–1231.
[19] H. Iikura, T. Nagata, *Inorg. Chem.* **1998**, *37*, 4702–4711.
[20] C. F. Wang, E. Q. Gao, Z. He, C. H. Yan, *Chem. Commun.* **2004**, 720–721.
[21] Y. Liu, V. Kravtsov, R. D. Walsh, P. Poddar, H. Srikanth, M. Eddaoudi, *Chem. Commun.* **2004**, 2806–2807.
[22] P. Sengupta, R. Dinda, S. Ghosh, W. S. Sheldrick, *Polyhedron* **2001**, *20*, 3349–3354.
[23] E. Colacio, J. M. Domínguez-Vera, M. Ghazi, R. Kivekäs, M. Klinga, J. M. Moreno, *Eur. J. Inorg. Chem.* **1999**, 441–445.
[24] C. Policar, F. Lambert, M. Cesario, I. Morgenstern-Badarau, *Eur. J. Inorg. Chem.* **1999**, 2201–2207.
[25] S. Durot, C. Policar, G. Pelosi, F. Bisceglie, T. Mallah, J. Mahy, *Inorg. Chem.* **2003**, *42*, 8072– 8080.
[26] H. Oshio, E. Ino, I. Magi, T. Ito, *Inorg. Chem.* **1993**, *32*, 5697–5703.
[27] E.-Q. Gao, L.-H. Yin, J.-K. Tang, P. Cheng, D.-Z. Liao, Z.-H. Jiang, S.-P. Yan, *Polyhedron* **2001**, *20*, 669–673.
[28] O. Kahn, *Molecular Magnetism*, VCH Publishers, New York, **1993**, p. 24.
[29] J. Cui, P. Cheng, D. Liao, Z. Jiang, S. Yan, G. Wang, X. Huang, *Polyhedron* **1998**, *17*, 2517–2522.
[30] R. Boća, *Coord. Chem. Rev.* **2004**, *248*, 757–815.

Received: October 2, 2005
Published Online: February 21, 2006

